



ELSEVIER

Oxamide oxime-based copper(II) coordination polymers. Two- and three-dimensional structures controlled by dicarboxylates[☆]

Satoshi Kawata, Susumu Kitagawa*, Hiroyuki Machida, Tadahiro Nakamoto, Mitsuru Kondo, Motomi Katada, Koichi Kikuchi, Isao Ikemoto

Department of Chemistry, Tokyo Metropolitan University, Hachioji 192-03, Japan

Received 14 June 1994

Abstract

The new Cu(II) complex, [Cu(H₂oao)(L(1,2))(H₂O)] (**1**), and coordination polymers, {[Cu(H₂oao)(L(2,4))]·H₂O}_n (**2**) and {[Cu(H₂oao)(Hoao)]·(HL(2,2))_n (**3**) (H₂oao = oxamide oxime; H₂L(1,2) = malic acid; H₂L(2,4) = succinic acid; H₂L(2,2) = maleic acid), have been synthesized and their structures have been X-ray crystallographically characterized. **1** crystallizes in the monoclinic, space group *P*2₁/*c* with *a* = 10.186(1), *b* = 6.648(1), *c* = 14.748(3) Å, β = 102.06(1)°, *U* = 976.5(3) Å³ and *Z* = 4. The mononuclear units in **1**, in which L(1,2)²⁻ chelates to Cu(II) ions, are linked to form a two-dimensional sheet structure through hydrogen bonds between coordinated H₂oao and L(1,2)²⁻. Additional hydrogen bonds link the layers to form a three-dimensional hydrogen bonding network. **2** crystallizes in the monoclinic, space group *P*2₁/*n* with *a* = 14.739(4), *b* = 9.994(3), *c* = 7.101(2) Å, β = 98.52(2)°, *U* = 1034.4(5) Å³ and *Z* = 4. The Cu(II) ions in **2** are bridged by L(2,4)²⁻ coordinated in an amphimonodentate mode, forming a one-dimensional zigzag chain. The water of crystallization is hydrogen bonded to both L(2,4)²⁻ and H₂oao of an adjacent chain, forming a two-layered sheet. Further weak hydrogen bonds link another chain, and an extended three-dimensional hydrogen bonding network runs through the crystal. **3** crystallizes in the monoclinic, space group *P*2₁/*c*, with *a* = 14.817(3), *b* = 13.693(4), *c* = 7.328(2) Å, β = 101.10(2)°, *U* = 1459.1(7) Å³ and *Z* = 4. In contrast to the case of **1** and **2**, the dicarboxylic acid, L(2,2)²⁻ in **3** is not coordinated to the Cu(II) ions. The axial coordination of the oximate oxygen in an adjacent Hoao to [Cu(H₂oao)(Hoao)]⁺ leads to the formation of a one-dimensional zigzag chain. The chains are linked by hydrogen bonds between H₂oao on adjacent chains to form sheets, which are sandwiched between uncoordinated HL(2,2)⁻ layers, resulting in a segregated double sheet structure in the crystal. The obtained structures are greatly associated with the size of the spacers, which link the carboxylate groups in the dicarboxylic acids, and hydrogen bonding interactions between the ligands.

Keywords: Crystal structures; Coordination polymers; Copper complexes; Oxamide complexes; Oxime complexes

1. Introduction

The infinite chain and sheet structures of metal complexes are of substantial interest in understanding the solid state chemistry of metal complexes [1–4]. Crystalline polymers having copper complex units provide not only novel structures and geometries, but also interesting magnetic and/or conductive properties [1–7]. However, from the synthetic point of view, there is a lack of literature elucidating the relationship between the polymer and monomer structures, which would help

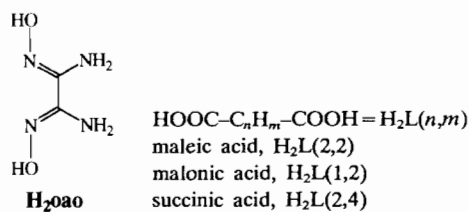
to rationalize the synthesis of copper complex polymers in the single crystal phase.

Compounds of transition metals with various kinds of 1,2-dione dioximes have been the objects of recent interest since the nature of the compounds formed in the solid state depends not only on the molecular structure but also on the crystal structure [5,8–24]. There are several chain compounds, which afford interesting electrical [1,19,20], optical [21,22] and magnetic properties [16]. In these series of compounds, oxime and/or oximate oxygen atoms have an important role in the dimensionality of the crystal structure. The three key factors controlling the crystal structure are bridging coordination, intermolecular and/or intramolecular types of hydrogen bonding, and the charged states of the monomer motifs obtained by the deprotonation of

[☆] This paper is dedicated to Professor F.A. Cotton on the occasion of his 65th birthday.

* Corresponding author.

the oxime groups. The hydrogen bonding is important for the realization of a three-dimensional architecture in a metal complex assembly [25–27]. This interaction is specific and directional and has little dependence on the properties of the metal ions, readily providing extended arrays [28,29]. Thus, one of the best strategies for the rational synthesis of coordination polymers is to utilize the hydrogen bondings of the coordinated ligands in addition to their linking capability. In this respect, oxamide oxime (H_2oao) is a good ligand for constructing coordination polymers as it has two kinds of proton donor atoms, oximate oxygens and amino nitrogens, which can form a multi-dimensional network of hydrogen bonding.



In addition to H_2oao several dicarboxylic acids with a C_nH_m spacer, which are capable of both chelating and bridging [30–34], have also been employed in order to extend the chemistry of transition metal–oxamide oxime compounds. We have succeeded in isolating three new types of mixed-ligand copper(II) compounds, $[Cu(H_2oao)(L(1,2))(H_2O)]$ (1), $\{[Cu(H_2oao)(L(2,4))] \cdot H_2O\}_n$ (2) and $\{[Cu(H_2oao)(Hoao)] \cdot (HL(2,2))\}_n$ (3), the crystal structures of which are primarily controlled by the spacer size of the dicarboxylic acids.

2. Experimental

2.1. Synthesis of 1

To an aqueous solution (2 ml) of $H_2L(1,2)$ (2×10^{-4} mol) were added aqueous solutions (2 ml) of $Cu(CH_3COO)_2 \cdot H_2O$ (1×10^{-4} mol) and H_2oao [35] (1×10^{-4} mol) with stirring. The green solution was filtered and allowed to stand at room temperature. Green plate crystals began to form within a week. One of these crystals was used for X-ray crystallography. *Anal.* Calc. for $CuC_5H_{10}N_4O_7$: C, 19.91; H, 3.34; N, 18.57. Found: C, 19.95; H, 3.38; N, 18.39%. IR (KBr pellet, cm^{-1}): 3222s, 3138s, 3099s, 2967m, 2925m, 1720m, 1683s, 1617s, 1588s, 1487m, 1453s, 1432s, 1407m, 1335s, 1284m, 1197m, 1058w, 1113w, 1058s, 1023m, 987m, 961m, 948w, 915w, 820s, 761m, 743m, 690m, 567m, 512m, 483w.

2.2. Synthesis of 2

To a saturated aqueous solution (2 ml) of $H_2L(2,4)$ (1×10^{-4} mol) were added aqueous solutions (2 ml)

of $Cu(CH_3COO)_2 \cdot H_2O$ (5×10^{-5} mol) and H_2oao (5×10^{-5} mol) with stirring. The green solution was filtered and allowed to stand at room temperature. Green plate crystals began to form in three days. One of these crystals was used for X-ray crystallography. *Anal.* Calc. for $CuC_6H_{12}N_4O_7$: C, 22.83; H, 3.83; N, 17.75. Found: C, 22.76; H, 3.78; N, 17.80%. IR (KBr pellet, cm^{-1}): 3525m, 3405s, 3363s, 3250s, 3200s, 2750m, 2530m, 1669s, 1613m, 1490s, 1431s, 1384s, 1215s, 1163m, 1161w, 1130w, 1077s, 1052m, 948w, 910m, 669s, 632mw, 567m, 500m, 458w.

2.3. Synthesis of 3

To an aqueous solution of $H_2L(2,2)$ (2 ml) were added aqueous solutions (2 ml) of $Cu(CH_3COO)_2 \cdot H_2O$ (5×10^{-5} mol) and H_2oao (5×10^{-5} mol) with stirring. The dark green solution was filtered and allowed to stand at room temperature. Within 3 days, black plate crystals began to form. One of these crystals was used for X-ray crystallography. *Anal.* Calc. for $CuC_8H_{14}N_8O_8$: C, 23.22; H, 3.41; N, 27.08. Found: C, 23.25; H, 3.46; N, 27.00%. IR (KBr pellet, cm^{-1}): 3432s, 3328s, 3214s, 3166s, 2768w, 1655s, 1583s, 1468s, 1384w, 1344s, 1196w, 1119w, 1038s, 969m, 923w, 860m, 747m, 705m, 563m, 499w.

2.4. Physical measurements

IR spectra of KBr discs were measured on a Hitachi I-5040FT-IR spectrophotometer. EPR spectra were recorded at X-band frequency with a JEOL RE-3X spectrometer operating at 9.1–9.5 GHz. Resonance frequency was measured on an Anritsu MF76A microwave frequency counter. Magnetic fields were calibrated by an Echo Electronics EFM-2000AX NMR field meter. The EPR spectra were recorded with a modulation frequency of 100 kHz and a modulation amplitude c mT, throughout. Magnetic susceptibility data were recorded over the temperature range 2–300 K at 1 T with a SQUID susceptometer (Quantum Design, San Diego, CA) interfaced with an HP Vectra computer system. All data were corrected for diamagnetism which was calculated from Pascal's table. TIP was assumed to be $60 \times 10^{-6} cm^3 mol^{-1}$. Least-squares fitting of the magnetic susceptibility to approximate equations for the antiferromagnetic chain (vide infra) were performed with the least-squares program NGRAPH on an NEC PC9801 computer.

2.5. Crystallographic data collection and refinement of the structure

A suitable crystal was chosen and mounted on a glass fiber with epoxy resin. Data collections were carried out on an Enraf-Nonius CAD-4 automated diffracto-

meter for **1**, and a MAC Science MXC18 automated diffractometer for **2** and **3**. The structures were solved by direct methods. Full-matrix least-squares refinements were carried out with anisotropic thermal parameters for all non-hydrogen atoms. All the hydrogen atoms were located in the Fourier difference maps. Hydrogen atoms of **1** were refined isotropically. The hydrogen atom coordinates for **2** were held fixed. The hydrogen atom coordinates of **3** were refined but their isotropic B values were held fixed. The final cycle of full-matrix least-squares refinement was based on N_o and n variable parameters and converged (large parameter shift was σ times its e.s.d.) with unweighted agreement factors of $R = \sum ||F_o| - |F_c|| / \sum |F_o|$, $R_w = [\sum (|F_o| - |F_c|)^2 / \sum w |F_o|^2]^{1/2}$ where $w = 4F_o^2 / \sigma^2(F_o^2)$.

2.5.1. Crystal data of **1**

$\text{CuO}_7\text{N}_4\text{C}_5\text{H}_{10}$, $M = 301.70$, monoclinic, space group $P2_1/c$, $a = 10.186(1)$, $b = 6.648(1)$, $c = 14.748(3)$ Å, $\beta = 102.06(1)^\circ$, $U = 976.5(3)$ Å³, $Z = 4$, $D_c = 2.05$ g cm⁻³, $\lambda(\text{Mo K}\alpha) = 0.71069$ Å, $F(000) = 572$, $\mu(\text{Mo K}\alpha) = 22.6$ cm⁻¹, $T = 20$ °C. Specimen size: $0.2 \times 0.1 \times 0.6$ mm. $2\theta_{\text{max}} = 52.6^\circ$; N , N_o ($I > 3\sigma(I)$) = 1979, 1732; $n = 194$; R , $R_w = 0.024$, 0.039. The final positional and equivalent thermal parameters are given in Table 1.

Table 1
Positional parameters and B_{eq} for $[\text{Cu}(\text{H}_2\text{oao})(\text{L}(1,2))(\text{H}_2\text{O})]$ (**1**)

Atom	x	y	z	B_{eq}
Cu	0.27354(2)	0.24014(3)	0.39357(1)	1.460(5)
O(1)	0.0506(1)	0.1644(3)	0.23147(9)	2.70(3)
O(2)	0.2104(1)	0.3140(3)	0.589065(9)	2.31(3)
O(3)	0.3211(1)	0.1571(3)	0.27989(8)	2.43(3)
O(4)	0.4548(1)	0.2386(2)	0.4651(1)	1.71(3)
O(5)	0.4524(1)	0.0503(2)	0.18982(8)	2.25(3)
O(6)	0.6727(2)	0.2197(2)	0.4762(1)	2.59(3)
O(7)	0.2970(1)	0.5794(2)	0.35519(9)	2.11(3)
N(1)	0.0889(2)	0.1958(3)	0.3266(1)	1.87(3)
N(2)	0.1699(2)	0.2848(2)	0.4935(1)	1.51(3)
N(3)	-0.1379(2)	0.2041(3)	0.3319(3)	2.59(4)
N(4)	-0.0425(2)	0.2473(2)	0.5274(1)	2.00(4)
C(1)	-0.0080(2)	0.2149(3)	0.3690(1)	1.44(3)
C(2)	0.0433(2)	0.2517(2)	0.4705(1)	1.32(3)
C(3)	0.4320(2)	0.0873(3)	0.2680(1)	1.53(3)
C(4)	0.5397(2)	0.0406(3)	0.3525(1)	1.75(3)
C(5)	0.5567(2)	0.1788(3)	0.4356(1)	1.54(3)
H(1)	0.110(2)	0.157(4)	0.217(2)	4.7(6)
H(2)	0.273(2)	0.364(4)	0.593(1)	2.6(5)
H(3)	-0.158(3)	0.188(4)	0.277(2)	3.7(6)
H(4)	-0.193(3)	0.228(3)	0.368(2)	3.8(7)
H(5)	-0.114(3)	0.228(3)	0.512(2)	3.5(6)
H(6)	-0.017(2)	0.258(3)	0.579(2)	1.7(5)
H(7)	0.511(2)	-0.085(3)	0.375(1)	2.5(4)
H(8)	0.621(2)	0.018(3)	0.334(1)	1.7(4)
H(9)	0.310(2)	0.648(4)	0.406(1)	2.9(5)
H(10)	0.370(2)	0.573(4)	0.341(2)	3.9(6)

Table 2
Positional parameters and B_{eq} for $\{[\text{Cu}(\text{H}_2\text{oao})(\text{L}(2,4))](\text{H}_2\text{O})\}_n$ (**2**)

Atom	x	y	z	B_{eq}
Cu	0.06657(3)	0.44154(4)	0.83314(7)	1.58(2)
O(1)	-0.1050(2)	0.2836(3)	0.6708(5)	2.40(7)
O(2)	0.2453(2)	0.2872(3)	0.9522(4)	2.29(7)
O(3)	0.1510(2)	0.5909(2)	0.9170(4)	1.74(6)
O(4)	0.2744(2)	0.5133(3)	1.1051(4)	2.72(7)
O(5)	-0.1217(2)	0.5207(3)	0.5244(4)	2.46(7)
O(6)	-0.0318(2)	0.5787(2)	0.7950(4)	1.82(6)
O(7)	0.0813(2)	0.8192(3)	0.7246(5)	2.52(7)
N(1)	-0.0121(2)	0.2866(3)	0.7420(4)	1.61(7)
N(2)	0.1519(2)	0.2892(3)	0.8852(4)	1.45(6)
N(3)	-0.0255(2)	0.0538(4)	0.7447(6)	2.44(8)
N(4)	0.1699(2)	0.0575(4)	0.8729(6)	2.48(8)
C(1)	0.0211(2)	0.1675(3)	0.7730(5)	1.44(8)
C(2)	0.1209(2)	0.1697(3)	0.8476(5)	1.36(7)
C(3)	-0.0952(2)	0.6025(3)	0.6552(5)	1.55(8)
C(4)	-0.1357(2)	0.7418(3)	0.6446(5)	1.44(8)
C(5)	0.2288(2)	0.6060(4)	1.0224(5)	1.52(7)
C(6)	0.2655(2)	0.7487(3)	1.0438(6)	1.47(8)

2.5.2. Crystal data of **2**

$\text{CuO}_7\text{N}_4\text{C}_6\text{H}_{12}$, $M = 315.72$, monoclinic, space group $P2_1/n$, $a = 14.739(4)$, $b = 9.994(3)$, $c = 7.101(2)$ Å, $\beta = 98.52(2)^\circ$, $U = 1034.4(5)$ Å³, $Z = 4$, $D_c = 2.03$ g cm⁻³, $\lambda(\text{Mo K}\alpha) = 0.71069$ Å, $F(000) = 604$, $\mu(\text{Mo K}\alpha) = 20.49$ cm⁻¹, $T = 23$ °C. Specimen size: $0.6 \times 0.2 \times 0.2$ mm. $2\theta_{\text{max}} = 60.0^\circ$; N , N_o ($I > 5\sigma(I)$) = 3010, 1807; $n = 164$; R , $R_w = 0.039$, 0.066. The final positional and equivalent thermal parameters are given in Table 2.

2.5.3. Crystal data of **3**

$\text{CuO}_8\text{N}_8\text{C}_8\text{H}_{14}$, $M = 413.79$, monoclinic, space group $P2_1/c$, $a = 14.817(3)$, $b = 13.693(4)$, $c = 7.328(2)$ Å, $\beta = 101.10(2)^\circ$, $U = 1459.1(7)$ Å³, $Z = 4$, $D_c = 1.88$ g cm⁻³, $\lambda(\text{Mo K}\alpha) = 0.71069$ Å, $F(000) = 596$, $\mu(\text{Mo K}\alpha) = 14.53$ cm⁻¹, $T = 23$ °C. Specimen size: $0.35 \times 0.20 \times 0.15$ mm. $2\theta_{\text{max}} = 55.0^\circ$; N , N_o ($I > 3\sigma(I)$) = 3346, 3048; $n = 269$; R , $R_w = 0.032$, 0.035. The final positional and equivalent thermal parameters are given in Table 3.

3. Results and discussion

3.1. Crystal structure of **1**

Fig. 1 shows an ORTEP drawing of the complex molecule. Bond distances and angles are listed in Table 4. The coordination environment of the copper ion is distorted square-pyramidal, with the basal plane being formed by two nitrogen atoms (N(1) and N(2)) of H_2oao and two oxygen atoms (O(3) and O(4)) of $\text{L}(1,2)^{2-}$. The $\text{L}(1,2)^{2-}$ ligand chelates to the copper atom, forming a six-membered ring. The oxygen atom (O(7)) of the water molecule occupies the apical position, the Cu–O bond length being 2.350(2) Å. The copper atom is

Table 3
Positional parameters and B_{eq} for $\{[\text{Cu}(\text{H}_2\text{oao})(\text{Hoao})](\text{HL}(2,2))\}_n$ (3)

Atom	x	y	z	B_{eq}
Cu	0.42352(2)	-0.14041(3)	0.00097(4)	1.686(9)
O(1)	0.4231(1)	-0.1994(1)	0.3939(2)	1.78(5)
O(2)	0.2526(2)	-0.0691(2)	-0.2633(3)	3.05(7)
O(3)	0.5620(2)	0.0563(2)	0.3738(3)	2.13(6)
O(4)	0.4120(1)	0.1826(2)	-0.2986(3)	2.08(5)
O(5)	-0.0879(2)	-0.0666(2)	0.3028(3)	3.72(7)
O(6)	0.0560(2)	-0.1009(2)	0.2922(3)	4.08(8)
O(7)	-0.1947(2)	-0.0923(2)	0.5084(4)	3.90(8)
O(8)	-0.1912(2)	-0.1583(2)	0.7827(4)	5.08(9)
N(1)	0.3723(2)	-0.1688(2)	0.2227(3)	1.77(6)
N(2)	0.2970(2)	-0.1004(2)	-0.0854(3)	2.12(6)
N(3)	0.5170(2)	0.0906(2)	0.1970(3)	1.76(6)
N(4)	0.4477(2)	0.1520(2)	-0.1168(3)	1.63(6)
N(5)	0.2423(2)	-0.1553(2)	0.3560(4)	2.87(8)
N(6)	0.1532(2)	-0.0815(3)	-0.0039(4)	3.33(9)
N(7)	0.3770(2)	0.0823(2)	0.3004(4)	2.40(7)
N(8)	0.2963(2)	0.1452(2)	-0.0740(4)	2.65(7)
C(1)	0.2874(2)	-0.1468(2)	0.2155(4)	1.76(7)
C(2)	0.2409(2)	-0.1066(2)	0.0305(4)	1.90(7)
C(3)	0.4291(2)	0.1008(2)	0.1754(4)	1.56(7)
C(4)	0.3861(2)	0.1360(2)	-0.0171(4)	1.56(6)
C(5)	-0.0098(2)	-0.1026(2)	0.3719(4)	2.56(8)
C(6)	0.0046(2)	-0.1492(3)	0.5597(5)	2.81(9)
C(7)	-0.0535(2)	-0.1616(3)	0.6750(5)	3.1(1)
C(8)	-0.1520(2)	-0.1354(3)	0.6552(5)	3.04(9)
H(1)	0.295(3)	-0.043(3)	-0.296(6)	
H(2)	0.566(3)	0.094(3)	0.443(5)	
H(3)	0.459(2)	0.189(3)	-0.336(5)	
H(4)	0.270(3)	-0.179(3)	0.446(5)	
H(5)	0.181(3)	-0.141(3)	0.346(5)	
H(6)	0.121(3)	-0.088(3)	0.075(6)	
H(7)	0.135(3)	-0.050(3)	-0.096(6)	
H(8)	0.402(3)	0.063(3)	0.394(5)	
H(9)	0.316(3)	0.100(3)	0.274(5)	
H(10)	0.259(3)	0.137(3)	-0.002(5)	
H(11)	0.279(3)	0.169(3)	-0.176(5)	
H(12)	-0.146(3)	-0.079(3)	0.406(6)	
H(13)	0.067(3)	-0.171(3)	0.604(5)	
H(14)	-0.030(3)	-0.191(3)	0.215(5)	

displaced from the mean basal plane (mean deviation from the plane is 0.0195 Å) by 0.14 Å. The two Cu–N bond distances are different (1.955(1), 2.006(2) Å), whereas the Cu–O distances are almost the same (1.921(1), 1.925(1) Å). The oxime ligand is not ionized and coordinates as a neutral ligand [13,15,36,37], in which one of the oxime groups forms an intramolecular hydrogen bond with $\text{L}(1,2)^{2-}$ (O(1)–O(3); 2.698(1) Å), resulting in the shorter Cu–N distance. A similar trend is found in the different Cu–N distances in $[\text{Cu}(\text{H}_2\text{oao})_2(\text{H}_2\text{O})]\text{SO}_4$ [16], which has an intramolecular hydrogen bond at the moiety having a shorter Cu–N bond. There are no intramolecular hydrogen bonds on the other side of the molecule, making the monomer motif asymmetric and providing a directional polymer structure.

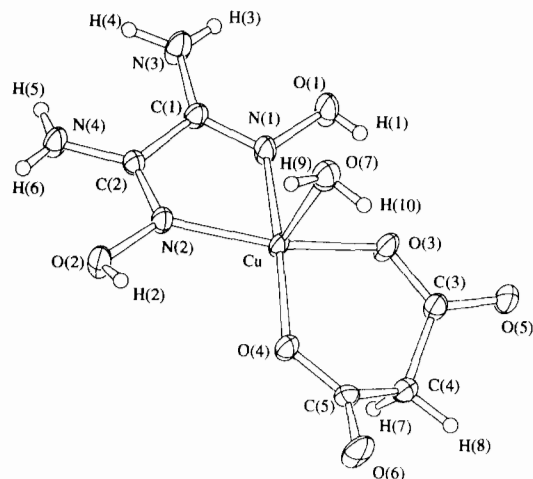


Fig. 1. ORTEP drawing of the asymmetric unit of compound 1 with labeling scheme and thermal ellipsoids at the 50% probability level for Cu, O, N and C atoms. Ellipsoids of the hydrogen atoms have been arbitrarily reduced.

As shown in Fig. 2, the O(1) atom on H_2oao is hydrogen bonded to both oxygen and nitrogen atoms of H_2oao on an adjacent molecule, the pairs of O(1)–N(4a) and O(1)–O(2a) being 3.018(2) Å, HB(1) and 2.917(2) Å, HB(2), respectively. The O(2a) atom is also hydrogen bonded to the oxygen (O(5)) of $\text{L}(1,2)^{2-}$ (2.751(2) Å, HB(3)). Further hydrogen bonds are formed between O(6) on $\text{L}(1,2)^{2-}$ and amino nitrogen atoms on H_2oao from the adjacent molecule, those being O(6)–N(3c) (3.159(4) Å, HB(4)) and O(6)–N(4c) (2.847(3) Å, HB(5)); then these hydrogen bond networks form a two-layered sheet. The apical water molecule is not only coordinated to the Cu(II) atom but also plays an additional role in linking the sheets. The hydrogen atoms of the water molecule are bound to the oxygen of $\text{L}(1,2)^{2-}$, and those of the amino nitrogen atoms on $\text{L}(1,2)^{2-}$ are bound to the water molecules, as shown in Fig. 2: the distances of O(5)–O(7b), O(6a)–O(7c) and N(3c)–O(7b) are 2.775(2), 2.782(2) and 3.010(4) Å, respectively. Compound 1 is, thus, a three-dimensional system, where all the coordinated ligands participate in hydrogen bonding networks. As far as this hydrogen bonding is concerned, the copper complex unit is a good motif for constructing a large structure in the crystal phase.

3.2. Crystal structure and magnetic properties of 2

An ORTEP drawing of the asymmetric unit of 2 with the atom numbering scheme is shown in Fig. 3, and selected bond distances and angles with their e.s.d.s are listed in Table 4. The geometry around the Cu(II) ion is approximately square planar involving the two nitrogen atoms (N(1), N(2)) of H_2oao as well as the oxygen atoms (O(3), O(6)) from two $\text{L}(2,4)^{2-}$. The Cu–N and Cu–O bond distances are in the range

Table 4
Selected bond distances (Å) and angles

Distances					
1					
Cu–O(3)	1.921(1)	O(4)–C(5)	1.271(2)	N(4)–C(2)	1.333(3)
Cu–O(4)	0.925(1)	O(5)–C(3)	1.237(2)	C(1)–C(2)	1.499(3)
Cu–N(1)	1.955(1)	O(6)–C(5)	1.238(2)	C(3)–C(4)	1.510(2)
Cu–N(2)	2.006(2)	N(1)–C(1)	1.280(3)	C(4)–C(5)	1.513(3)
O(2)–N(2)	1.397(2)	N(2)–C(2)	1.282(2)	Cu–O(7)	2.350(2)
O(3)–C(3)	1.268(2)	N(3)–C(1)	1.324(2)		
2^a					
Cu–N(1)	1.985(3)	N(1)–C(1)	1.293(4)	C(5)–O(4)	1.240(4)
Cu–N(2)	1.974(3)	N(1)–O(1)	1.388(4)	C(5)–C(6)	1.525(5)
Cu–O(3)	1.978(2)	N(2)–C(2)	1.292(4)	Cu...O(5a)	2.804(3)
Cu–O(6)	1.985(2)	C(1)–N(3)	1.328(5)	Cu...O(6b)	2.770(3)
O(2)–N(2)	1.389(4)	C(2)–N(4)	1.332(5)	Cu–Cu(a)	4.985(1)
O(3)–C(5)	1.282(4)	C(2)–C(1)	1.448(4)	Cu–Cu(b)	3.494(1)
O(5)–C(3)	1.255(4)	C(3)–C(4)	1.513(5)	Cu–Cu(c)	9.858(2)
O(6)–C(3)	1.280(4)	C(4)–C(6)	1.528(4)		
3^b					
Cu–N(1)	1.960(2)	O(7)–C(8)	1.282(4)	C(1)–C(2)	1.502(4)
Cu–N(2)	1.939(2)	O(8)–C(8)	1.232(5)	C(3)–C(4)	1.511(4)
Cu–N(3)	1.959(2)	N(1)–C(1)	1.285(4)	C(6)–C(7)	1.328(5)
Cu–N(4)	1.939(2)	N(2)–C(2)	1.300(4)	C(6)–C(5)	1.495(5)
O(1)–N(1)	1.397(3)	N(3)–C(3)	1.290(4)	C(8)–C(7)	1.482(5)
O(2)–N(2)	1.409(3)	N(4)–C(4)	1.294(4)	Cu–O(1a)	2.329(2)
O(3)–N(3)	1.418(3)	N(5)–C(1)	1.336(4)	Cu–Cu(b)	4.465(1)
O(4)–N(4)	1.400(3)	N(6)–C(2)	1.320(4)	Cu–Cu(c)	4.736(1)
O(5)–C(5)	1.270(4)	N(7)–C(3)	1.330(4)		
O(6)–C(5)	1.230(4)	N(8)–C(4)	1.322(4)		
Angles					
1					
O(3)–Cu–O(4)	95.11(6)	N(1)–C(1)–N(3)	126.8(2)		
O(3)–Cu–N(1)	84.65(6)	N(1)–C(1)–C(2)	111.1(2)		
O(3)–Cu–N(2)	162.00(6)	N(3)–C(1)–C(2)	122.1(2)		
O(4)–Cu–N(1)	170.72(7)	N(2)–C(2)–N(4)	126.4(2)		
O(4)–Cu–N(2)	100.94(6)	N(2)–C(2)–C(1)	114.4(2)		
N(1)–Cu–N(2)	78.19(6)	N(4)–C(2)–C(1)	119.2(2)		
Cu–O(3)–C(3)	128.4(1)	O(3)–C(3)–O(5)	122.0(1)		
Cu–O(4)–C(5)	124.9(1)	O(3)–C(3)–C(4)	118.4(2)		
Cu–N(1)–O(1)	124.7(1)	O(5)–C(3)–C(4)	119.6(2)		
Cu–N(1)–C(1)	119.8(1)	C(3)–C(4)–C(5)	118.9(2)		
Cu–N(2)–O(2)	132.2(1)	O(4)–C(5)–O(6)	122.1(2)		
Cu–N(2)–C(2)	115.8(1)	O(4)–C(5)–C(4)	120.3(1)		
O(1)–N(1)–C(1)	115.2(1)	O(6)–C(5)–C(4)	117.5(2)		
O(2)–N(2)–C(2)	111.1(2)				
2					
N(2)–Cu–O(3)	99.8(1)	N(2)–C(2)–N(4)	125.6(3)		
N(2)–Cu–O(6)	172.0(1)	N(2)–C(2)–C(1)	112.8(3)		
N(2)–Cu–N(1)	77.5(1)	N(4)–C(2)–C(1)	121.6(3)		
O(3)–Cu–O(6)	86.2(1)	O(5)–C(3)–O(6)	124.4(3)		
O(3)–Cu–N(1)	176.5(1)	O(5)–C(3)–C(4)	119.0(3)		
O(6)–Cu–N(1)	96.6(1)	O(6)–C(3)–C(4)	116.5(3)		
C(1)–N(1)–O(1)	111.7(3)	O(4)–C(5)–O(3)	124.3(3)		
C(2)–N(2)–O(2)	111.1(3)	O(4)–C(5)–O(6)	119.5(3)		
N(1)–C(1)–N(3)	126.0(3)	O(3)–C(5)–C(6)	116.2(3)		
N(1)–C(1)–C(2)	112.1(3)	C(3)–O(6)–Cu	131.9(2)		
N(3)–C(1)–C(2)	121.9(3)	C(5)–O(3)–Cu	137.1(2)		
3					
N(2)–Cu–N(1)	79.8(1)	N(1)–C(1)–N(5)	125.4(2)		
N(2)–Cu–N(4)	166.9(1)	N(1)–C(1)–C(2)	113.4(2)		
N(2)–Cu–N(3)	101.8(1)	N(5)–C(1)–C(2)	121.2(2)		
N(1)–Cu–N(4)	97.25(9)	N(2)–C(2)–N(6)	126.0(3)		
N(1)–Cu–N(3)	169.7(1)	N(2)–C(2)–C(1)	112.0(2)		

(continued)

Table 4 (continued)

Angles			
3			
N(4)–Cu–N(3)	78.92(9)	N(6)–C(2)–C(1)	122.1(3)
C(1)–N(1)–O(1)	117.4(2)	N(3)–C(3)–N(7)	127.0(2)
C(1)–N(1)–Cu	116.9(2)	N(3)–C(3)–C(4)	112.5(2)
O(1)–N(1)–Cu	125.2(2)	N(7)–C(3)–C(4)	120.5(2)
C(2)–N(2)–O(2)	112.4(2)	N(4)–C(4)–N(8)	125.7(2)
C(2)–N(2)–Cu	117.9(2)	N(4)–C(4)–C(3)	111.4(2)
O(2)–N(2)–Cu	129.6(2)	N(8)–C(4)–C(3)	122.9(3)
C(3)–N(3)–O(3)	115.7(2)	C(7)–C(6)–C(5)	130.2(3)
C(3)–N(3)–Cu	117.4(2)	O(6)–C(5)–O(5)	123.3(3)
O(3)–N(3)–Cu	126.4(2)	O(6)–C(5)–C(6)	117.4(3)
C(4)–N(4)–O(4)	114.2(2)	O(5)–C(6)–C(6)	119.3(3)
C(4)–N(4)–Cu	118.7(2)	O(8)–C(8)–O(7)	121.6(3)
O(4)–N(4)–Cu	126.9(2)	O(8)–C(8)–C(7)	117.6(3)
C(13)–C(7)–C(8)	130.8(3)	O(7)–C(8)–C(7)	120.8(3)
Hydrogen bond distances and angles			
1^c			
O(1)–O(3)	2.698(1)	O(1)–H(1)–O(3)	137.0
O(1)–N(4a) (HB(1))	3.018(2)	O(1)–H(6a)–N(4a)	172.0
O(1)–O(2a) (HB(2))	2.917(2)	O(1)–H(1)–O(2a)	144.0
O(2a)–O(5) (HB(3))	2.751(2)	O(2a)–H(2a)–O(5)	143.4
O(5)–O(7b)	2.775(2)	O(5)–H(10b)–O(7b)	178.0
O(6a)–O(7b)	2.782(2)	O(6a)–H(9b)–O(7b)	174.0
O(6)–N(3c) (HB(4))	3.159(4)	O(6)–H(4c)–N(3c)	167.1
O(6)–N(4c) (HB(5))	2.847(3)	O(6)–H(5c)–N(4c)	170.5
O(7b)–N(3c)	3.010(4)	O(7b)–H(3c)–N(3c)	153.1
2^a			
O(1)–O(5)	2.585(4)	O(1)–H(1)–O(5)	167.0
O(2)–O(4)	2.516(4)	O(2)–H(8)–O(4)	101.0
N(3d)–O(7)	2.839(4)	N(3d)–H(4d)–O(7)	152.9
N(4d)–O(7)	2.842(4)	N(4d)–H(5d)–O(7)	167.3
O(1a)–O(7)	3.058(4)	O(1a)–H(11)–O(7)	148.4
O(2c)–O(7)	3.027(3)	O(2c)–H(11)–O(7)	138.9
O(3)–O(7)	2.777(2)	O(3)–H(12)–O(7)	158.1
O(6)–O(7)	3.009(3)	O(6)–H(12)–O(7)	127.5
3^b			
O(1)–O(4)	2.677(2)	O(1)–H(3)–O(4)	172.8
O(2)–O(3)	3.015(4)	O(2)–H(2)–O(3)	134.0
O(5)–O(7)	2.412(4)	O(5)–H(12)–O(7)	175.8
O(3)–O(1d)	2.577(3)	O(3)–H(2)–O(1d)	175.1
O(3)–N(7e)	3.048(4)	O(3)–H(8)–N(7e)	154.0
N(5)–O(6)	2.810(4)	N(5)–H(5)–O(6)	171.3
N(6)–O(6)	2.838(4)	N(6)–H(6)–O(6)	173.0
N(7)–O(8f)	2.896(4)	N(7)–H(9)–O(8f)	171.5
N(8)–O(8f)	2.880(5)	N(8)–H(10)–O(8f)	160.3

^a Symmetry codes: a: $-x, -y, -z$; b: $-x, 1-y, 2-z$; c: $\frac{1}{2}+x, \frac{3}{2}-y, \frac{1}{2}+z$; d: $x, 1+y, z$; e: $\frac{1}{2}-x, \frac{1}{2}+y, \frac{3}{2}-z$.

^b Symmetry codes: a: $x, -\frac{1}{2}-y, \frac{1}{2}+z$; b: $x, \frac{1}{2}-y, \frac{1}{2}+z$; c: $x, \frac{1}{2}-y, -\frac{1}{2}+z$; d: $x, y, 1+z$; e: $1-x, -y, -1-z$; f: $-1+x, y, 1+z$.

^c Symmetry codes: a: $x, \frac{1}{2}-y, -\frac{1}{2}+z$; b: $2-x, -1+y, \frac{1}{2}-z$; c: $x+1, y, z$.

1.974(3)–1.985(3) Å, comparable to those of related complexes [13,15,30,32,36,37]. The Cu–N distances are close to each other, unlike in **1**, affording a symmetrical coordination geometry around the copper atom. The crystal structure comprises a zigzag chain linked by amphimonodentate succinate dianions. The dicarboxylic acid having a long methylene spacer prefers bridging to chelating, thus providing a one-dimensional chain.

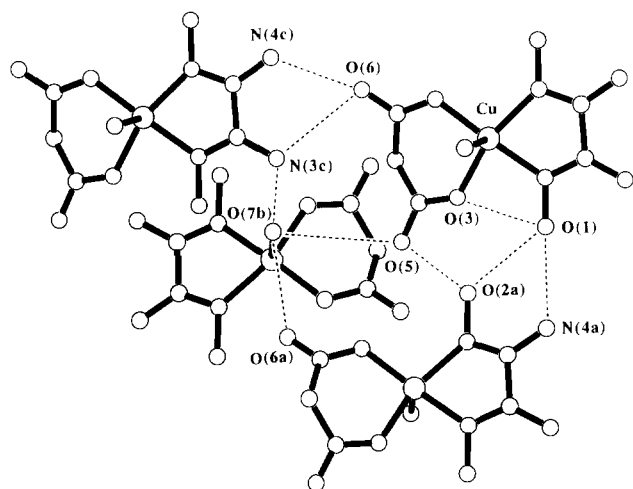


Fig. 2. Projection of the layers of compound 1 along the *b* axis. The dashed lines denote the sites of hydrogen bonding between the molecules.

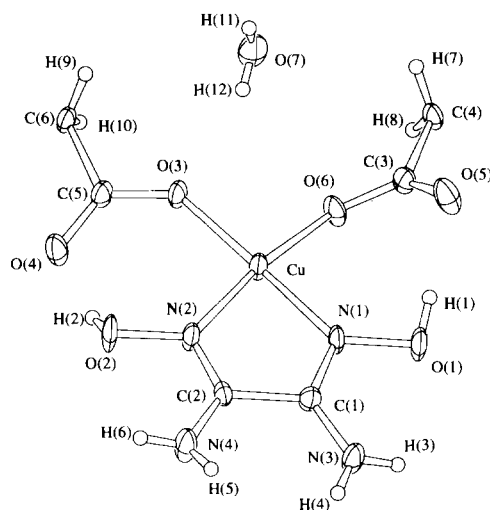


Fig. 3. ORTEP drawing of the asymmetric unit of compounds 2 with labeling scheme and thermal ellipsoids at the 50% probability level for Cu, O, N and C atoms. Ellipsoids of the hydrogen atoms have been arbitrarily reduced.

The projection view on the *ab* plane is given in Fig. 4(a). The repeating unit of $\text{Cu}(\text{H}_2\text{oao})(\text{L}(2,4))$ develops along the *ab* plane. The chains are in close contact: the shortest interchain metal–metal distance is 3.494(1) Å, while intrachain nearest-neighbor Cu–L(2,4)–Cu is 9.858(2) Å. The interchain interaction exists as the formation of semicoordinate bonds between the copper atom and carboxyl oxygens on $\text{L}(2,4)^{2-}$ (O(5), O(6)), the distances being 2.804(3) and 2.771(3) Å, respectively, affording alternating bridging between the copper atoms on adjacent chains (Fig. 4(b)). The large difference of 0.04 Å between the C–O distances (C(5)–O(3), C(5)–O(4)), implying a partial double bond character of the C(5)–O(4) bond, is in line with the coordination mode of the carboxylate groups, while the difference between the C–O distances in the other carboxylate

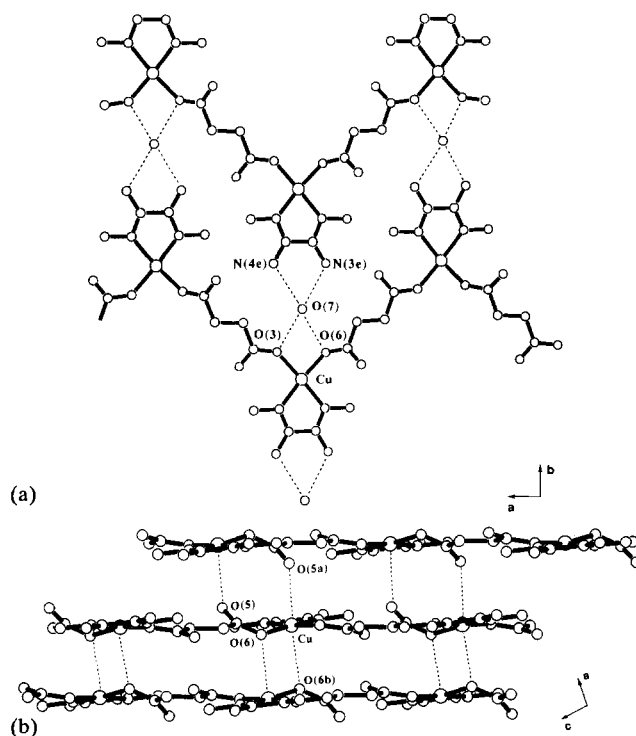


Fig. 4. (a) View onto the *ab* plane of a layer of compound 2. The dashed lines denote the sites of hydrogen bonding between the molecules. (b) View onto the *ac* plane of chains of compound 2 without the water of crystallization. The dashed lines denote the semicoordinate bonds.

(C(3)–O(5), C(3)–O(6)) is small in accordance with the axial interaction.

The polycrystalline powder EPR at 6 K appears axial ($g_{\parallel} = 2.290$, $g_{\perp} = 2.064$), as expected for a Cu(II) ion with a $d_{x^2-y^2}$ ground state. No hyperfine structure was observed, however the linewidth appeared to be extremely narrow suggesting the presence of significant exchange narrowing [38]. Magnetic susceptibilities (χ_M) were measured over the temperature range 2–300 K. $\chi_M T$ decreases at lower temperatures indicative of the presence of a weak antiferromagnetic exchange coupling in the crystal (Fig. 5). Data were analyzed using the Heisenberg linear chain theory¹, to give the fitting with

¹ The equation for an isolated $S = 1/2$, antiferromagnetic chain is

$$\chi' = \left(\frac{Ng^2 \mu_B^2}{kT} \right) \frac{A + Bx + Cx^2}{1 + Dx + Ex^2 + Fx^3} \quad (1)$$

where $x = |J|/kT$, $A = 0.25$, $B = 0.14995$, $C = 0.30094$, $D = 1.9862$, $E = 0.68854$, $F = 6.0626$, J is the intrachain-exchange-coupling constant and other symbols have their usual meaning. When J is negative, the exchange is antiferromagnetic. Interchain exchange interaction was accounted for by the addition of a mean field correction term to Eq. (1). The equation for the susceptibility then has the form;

$$\chi = \frac{\chi'}{1 - 2zJ'\chi'/Ng^2 \mu_B^2} (1 - \rho) + \rho \frac{Ng^2 \mu_B^2}{4kT} + N\alpha \quad (2)$$

where z is the number of near neighbors in adjacent chains, J' is the interchain exchange parameter, ρ is the fraction of monomeric impurity, and $N\alpha$ is TIP [39].

$J = -2.35 \text{ cm}^{-1}$, $zJ' = -0.86 \text{ cm}^{-1}$, $g = 2.20$, $\rho = 3.82\%$ and R (agreement factor) $= 5.96 \times 10^{-5}$. It may indicate a two-dimensional exchange interaction spread over the polymer. However, we cannot determine whether the effective exchange pathway is inter- or intrachain. The absolute value of J is large compared to those of the dinitroxyl radicals ($J = 0.25$ and $-25 \times 10^{-4} \text{ cm}^{-1}$), which have radical–radical distances of 9 and 11 Å, respectively [40]. Since the Cu–Cu distance within the chain is too long and there are seven bonds between the copper atoms, in which three of them are saturated C–C bonds in bridging $L(2,4)^{2-}$, interchain interactions are anticipated [41]. There are two kinds of apical interactions around the Cu(II) atom: Cu–O(6)–Cu and Cu–O(5)–C(3)–O(6)–Cu. The former type of interaction is found in the parallel planar dimer [42,43], and the latter type configuration of its carboxylato bridge is also seen in copper carboxylate derivatives [32,44,45]. In all cases, the magnitudes of the exchange coupling constants are small. Owing to the symmetry of the bridging network, the contributions of the orbitals on the oxygen atoms of $L(2,4)^{2-}$, belonging to the magnetic orbitals centered on the two successive copper atoms, are unfavorably oriented to give a strong overlap, accounting for the weak antiferromagnetism of **2**.

The geometry of H_2Oao is different to that in **1**. There are two intrachain hydrogen bonds formed between oxygens of H_2Oao and uncoordinated oxygens of $L(2,4)^{2-}$, being O(1)–O(5) (2.585(4) Å) and O(2)–O(4) (2.516(4) Å). Distances and angles of the hydrogen bonds are shown in Table 4. The oxygen atom (O(7)) of the water is hydrogen bonded to both the coordinated oxygens of $L(2,4)^{2-}$ (O(3), 2.777(2) Å; O(6), 3.009(3) Å) by unsymmetrical X-bifurcated-type bonding [46] and the amino nitrogens on H_2Oao (N(3d), 2.839(4) Å; N(4d), 2.842(4) Å) of an adjacent chain, forming a two-dimensional layer (Fig. 4(a)). Further X-bifurcated hydrogen bonds link the oximate oxygens (O(1a), 3.058(4) Å; O(2e), 3.027(3) Å) of another chain. Thus, the coordinated water is engaged in hydrogen bonds to different layers, and an extended three-dimensional hydrogen bonding network runs through the crystal.

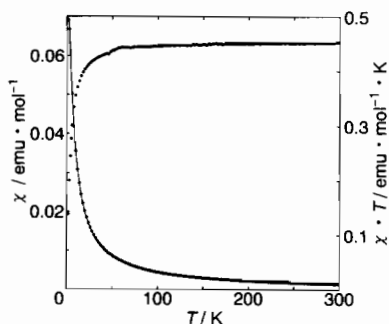


Fig. 5. Plots of $\chi_M T$ and χ_M vs. T . Solid line: theoretical fit of the data with the parameters listed in the text.

The one-dimensional zigzag chain compound of **2**, in which the dicarboxylic acid, $L(2,4)^{2-}$ is employed in the bridging ligand, thus weakly interacts three dimensionally by hydrogen bonding and semicoordination.

3.3. Crystal structure of **3**

An ORTEP drawing of the asymmetric unit of **3** with the atom numbering scheme is shown in Fig. 6, and selected bond distances and angles with their e.s.d.s are listed in Table 4. The Cu(II) ion has a slightly distorted square-pyramidal surrounding with the four basal nitrogen atoms of H_2Oao and $Hoao^-$ and the apical oxygen atom (O(1a)) of the nearest-neighbor $Hoao^-$. The Cu–O(1a) distance is 2.329(2) Å, shorter than that of **1**. This is because the copper atom deviates from the mean basal plane (mean deviation from the plane is 0.0251 Å) by 0.19 Å. The Cu–O(1a) type bond is available for the formation of a one-dimensional zigzag chain. The repeating unit of $Cu(H_2Oao)(Hoao)$ develops along the bc plane (Fig. 7(a)), in which the chains are close to each other: the shortest interchain Cu–Cu distance is 4.465(1) Å, while the intrachain nearest-neighbor Cu–Cu distance is 4.736(1) Å. This is clearly different from the case of **1** and **2**; the dicarboxylic acid monoanion $HL(2,2)^-$ is not coordinated to the Cu(II) ion, and serves as a counter anion of the complex.

H_2Oao is coordinated as a neutral ligand, while $Hoao^-$ is a mono deprotonated anion resulting in a monocationic complex fraction. The Cu–N bond distances (1.939(2)–1.960(2) Å) are similar to those found in complexes having two intramolecular hydrogen bonds between two oxime ligands [11]. Intramolecular hydrogen bonds are also found in **2**, that being O(1)–O(4) (2.677(2) Å) and O(2)–O(3) (3.015(4) Å). Distances and angles of the hydrogen bonds are shown in Table 4. The occurrence of two different O–O separations is ascribed to the large negativity of the oximate oxygen (O(1)) on $Hoao^-$, similar to those found in $[Ni(H_2Oao)(Hoao)]_2 \cdot (C_4O_4)$ [14]. The oxygen atom (O(3)) of H_2Oao is also hydrogen bonded to O(1d) (O(1d)–O(3), 2.577(3) Å) of $Hoao^-$ from the next neighbor monomer fraction and N(7e) (N(7e)–O(3),

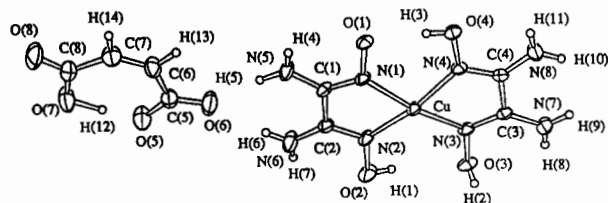


Fig. 6. ORTEP drawing of the asymmetric unit of compound **3** with labeling scheme and thermal ellipsoids at the 50% probability level for Cu, O, N and C atoms. Ellipsoids of the hydrogen atoms have been arbitrarily reduced.

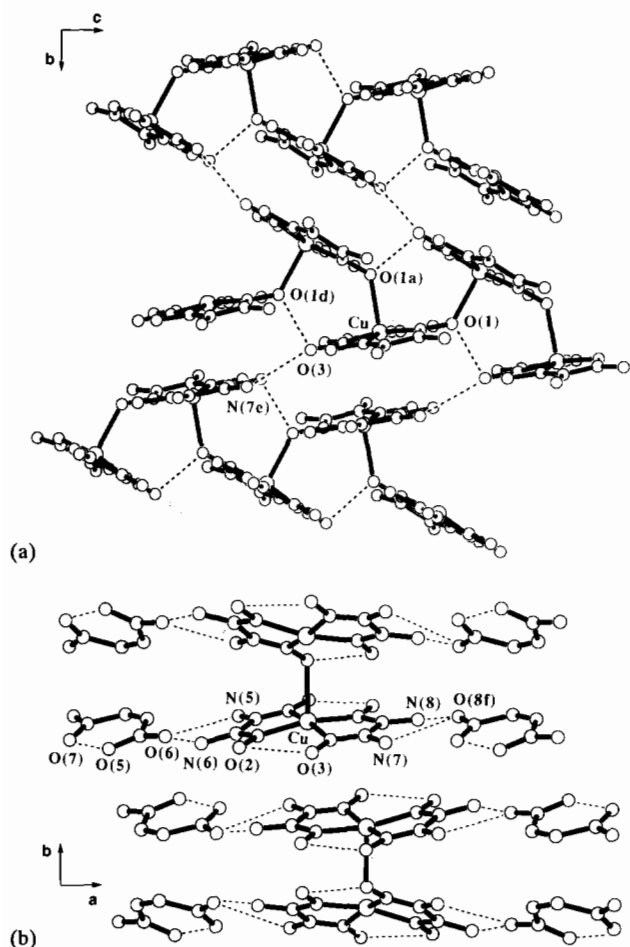


Fig. 7. (a) Layer structure of compound 3 without counter anion, $\text{HL}(2,2)^{-}$ projected down the a axis. The dashed lines denote the sites of hydrogen bonding. (b) View onto the ac plane of stacks of compound 3. The dashed lines denote the sites of hydrogen bonding.

$3.048(4) \text{ \AA}$) in the adjacent chain, resulting in the sheets (Fig. 7(a)).

Interestingly, $\{[\text{Cu}(\text{H}_2\text{oao})(\text{Hoao})]^+\}_n$ layers are sandwiched between uncoordinated $\text{HL}(2,2)^{-}$ which adopt the *cis* configuration and form layers. Thus the segregated double layered structure is formed as shown in Fig. 7(b) [18,47]. The dihedral angle between the basal plane of the $[\text{Cu}(\text{H}_2\text{oao})(\text{Hoao})]^+$ monomer fraction and the anion is about 10° , which is greater than the value for $[\text{Ni}(\text{H}_2\text{oao})_2] \cdot (\text{C}_4\text{O}_4)$ [14], due to the asymmetric structure of the anion. The anion has a planar structure not only because of the strong intramolecular hydrogen bond ($\text{O}(5) \cdots \text{O}(7)$, $2.412(4) \text{ \AA}$) but also due to the double bond of the ethylene linkage, resulting in layers consisting of the stacked anions. The *cis* type configuration of $\text{HL}(2,2)^{-}$, therefore, does not allow it to coordinate to the copper atom and to stack to form layers, as distinct from the bridging ligand $\text{L}(2,4)^{2-}$ whose spacer chain is saturated and flexible, indicating that the π -system of the spacer plays an important role in stabilizing the structure. Moreover, the amino nitrogen atoms of Hoao^- ($\text{N}(4)$ and $\text{N}(5)$)

and those of H_2oao are hydrogen bonded to the oxygens of $\text{HL}(2,2)^{-}$ ($\text{O}(6)$ and $\text{O}(8f)$, respectively), then uncoordinated oxygen atoms of $\text{HL}(2,2)^{-}$ work the proton acceptors of the amino groups on the metal complex like that of $\text{L}(1,2)^{2-}$ in 1, and $\text{HL}(2,2)^{-}$ layers are engaged in hydrogen bonds to the layers of the complexes. The uncoordinated dicarboxylic acid $\text{HL}(2,2)^{-}$ thus plays an important role in the formation of the two-dimensional structure of 3 through the hydrogen bonding interaction. Incorporation of organic molecules as counter anions into these metal- H_2oao systems by partially removing protons could result in the formation of ordered arrays of metal complexes.

3.4. Effect of the coordinated ligands on the crystal structures

The molecular assemblies of oxamide oxime-based $\text{Cu}(\text{II})$ complexes obtained here reveal the three key factors that control the crystal structure. The most important factor is the coordination mode of the dicarboxylic acids as well as the metal-free form. This makes the structural chemistry of copper(II)- $\text{oao}/\text{H}_n\text{oao}$ compounds fruitful. Compound 1 is not a coordination polymer but a monomeric mixed-ligand complex. The six-membered chelate coordination of the $\text{L}(1,2)^{2-}$ ligand is favored over the bridging coordination. The mode of coordination depends on the size of the spacer chains. Compound 2 demonstrates the bridging coordination of a dicarboxylic acid, $\text{L}(2,4)^{2-}$, which has one more methylene group than $\text{L}(1,2)^{2-}$. This is a typical coordination polymer of zigzag chains. When the conformation of the ligand is fixed, such as *cis*- $\text{HL}(2,2)^{-}$, which has a strong intramolecular hydrogen bond, no modes of chelation are possible nor any participation of the ligand to the molecular structure is expected. The obtained units are, thus, bis-chelated $[\text{Cu}(\text{H}_2\text{oao})(\text{Hoao})]^+$. Although the monomers are linked to each other to give infinite chains, compound 3 contains $\text{HL}(2,2)^{-}$ as a counter anion, providing anionic segregated columns. This is of interest for the construction of a reversible proton transfer system. The proton of $\text{HL}(2,2)^{-}$ and electronegative atoms of the cationic copper polymers are not located close enough for proton transfer to take place, but this structure is promising in this respect.

Another important point is the deprotonation of oxamide oxime, giving the neutral (H_2oao) and monovalent (Hoao^-) forms. The residual protons are involved preferentially in intramolecular hydrogen bonding, and furthermore the intermolecular hydrogen bonding occurs in the oxime oxygen atoms. In addition to the hydrogen bonding the charged states of the copper complexes are important for constructing crystal structures, which are dependent on the counter anions used.

Finally, hydrogen bonding between H₂O and other molecules such as dicarboxylates is significant. In compounds 1–3, the O–H...O distances range from 2.52 to 3.06 Å, while those of O–H...N or O...H–N fall within the range 2.81–3.16 Å. This hydrogen bonding in the crystal means that the monomeric and/or polymeric copper complexes are tightly linked and well-assembled. The hydrogen bonding increases the dimensionality of the system and thus provides structural varieties in the crystal structure.

Acknowledgements

This work was supported in part by a Grant-in-Aid for Scientific Research (No. 05453046) from the Ministry of Education, Science and Culture of Japan. We thank the Ciba-Geigy Foundation (Japan) for the Promotion of Science.

References

- [1] J.S. Miller (ed.), *Extended Linear Chain Compounds*, Plenum, New York, 1983.
- [2] P. Delhaes and M. Drillon (eds.), *Organic and Inorganic Low Dimensional Crystalline Materials*, Reidel, Dordrecht, Netherlands, 1987.
- [3] D. Gatteschi, O. Kahn, J.S. Miller and F. Palacio (eds.), *Magnetic Molecular Materials*, Reidel, Dordrecht, Netherlands, 1991.
- [4] D.W. Bruce and D. O'Hare (eds.), *Inorganic Materials*, Wiley, Chichester, UK, 1992.
- [5] R.D. Willet, D. Gatteschi and O. Kahn (eds.), *Magneto-Structural Correlation in Exchange-Coupled Systems*, Reidel, Dordrecht, Netherlands, 1985.
- [6] D. Segal, *Chemical Synthesis of Advanced Ceramic Materials*, Cambridge University Press, Cambridge, UK, 1989.
- [7] O. Kahn, *Molecular Magnetism*, VCH, New York, 1993.
- [8] H. Endres, H.J. Keller, W. Moroni and J. Weiss, *Acta Crystallogr., Sect. B*, 31 (1975) 2357.
- [9] H. Endres, *Acta Crystallogr., Sect. B*, 35 (1979) 3032.
- [10] H. Endres and T. Jannack, *Acta Crystallogr., Sect. B*, 36 (1980) 2136.
- [11] H. Endres, N. Genc and D. Nöthe, *Acta Crystallogr., Sect. C*, 39 (1983) 701.
- [12] H. Endres and N. Genc, *Acta Crystallogr., Sect. C*, 39 (1983) 704.
- [13] H. Endres, *Acta Crystallogr., Sect. C*, 39 (1983) 1192.
- [14] H. Endres and M. Schendzielorz, *Acta Crystallogr., Sect. C*, 39 (1983) 1528.
- [15] H. Endres, N. Genc and D. Nöthe, *Z. Naturforsch., Teil B*, 38 (1983) 90.
- [16] H. Endres, D. Nöthe, E. Rossato and W.E. Hatfield, *Inorg. Chem.*, 23 (1984) 3467.
- [17] H. Endres, *Angew. Chem., Int. Ed. Engl.*, 23 (1984) 999.
- [18] H. Endres, A. Bongart, D. Nöthe and B. Rosenau, *Z. Naturforsch., Teil B*, 41 (1986) 334.
- [19] M. Cowie, A. Gleizes, G.W. Grynkewich, D.W. Kalina, M.S. McClure, R.P. Scaringe, R.C. Teitelbaum, S.L. Ruby, J.A. Ibers, C.R. Kannewurf and T.J. Marks, *J. Am. Chem. Soc.*, 101 (1979) 2921.
- [20] L.D. Brown, D.W. Kalina, M.S. McClure, S. Schultz, S.L. Ruby, J.A. Ibers, C.R. Kannewurf and T.J. Marks, *J. Am. Chem. Soc.*, 101 (1979) 2937.
- [21] I. Shirovani, K. Suzuki, T. Suzuki, T. Yagi and M. Tanaka, *Bull. Chem. Soc. Jpn.*, 65 (1992) 1078.
- [22] I. Shirovani, K. Suzuki and T. Yagi, *Proc. Jpn. Acad.*, 68B (1992) 57.
- [23] H. Ojima and K. Nonoyama, *Coord. Chem. Rev.*, 92 (1988) 85.
- [24] R. Ruiz, J. Sanz, B. Cervera, F. Lloret, M. Julve, C. Bois, J. Faus and M.C. Muñoz, *J. Chem. Soc., Dalton Trans.*, (1993) 1623.
- [25] C. Robl and W. Kuhs, *J. Solid State Chem.*, 75 (1988) 15.
- [26] C. Robl, S. Hentschel and G. McIntyre, *J. Solid State Chem.*, 96 (1992) 318.
- [27] S.R. Breeze and S. Wang, *Inorg. Chem.*, 32 (1993) 5981.
- [28] T. Zeegers-Huyskens and P.L. Huyskens, in P.L. Huyskens, A.P. Luck and T. Zeegers-Huyskens (eds.), *Intermolecular Forces – an Introduction to Modern Methods and Results*, Springer, Berlin, 1991.
- [29] C.B. Aakeröy and K.R. Seddon, *Chem. Soc. Rev.*, (1993) 397.
- [30] B.H. O'Connor and E.N. Maslen, *Acta Crystallogr.*, 20 (1966) 824.
- [31] C.T. Dziobkowski, J.T. Wroblewski and D.B. Brown, *Inorg. Chem.*, 20 (1981) 671.
- [32] E. Bakalbassis, C. Tsipis, A. Bozopoulos, W. Dreissig, H. Hartl and J. Mrozinski, *Inorg. Chim. Acta*, 186 (1991) 113.
- [33] C.E. Xanthopoulos, M.P. Sigalas, G. Katsoulos A., C.A. Tsipis, A. Terzis, M. Mentzafos and A. Hountas, *Inorg. Chem.*, 32 (1993) 5433.
- [34] T. Kiss, G. Micera, D. Sanna and H. Kozłowski, *J. Chem. Soc., Dalton Trans.*, (1994) 347.
- [35] J.G.A. Pearce and R.T. Pfraum, *J. Am. Chem. Soc.*, 81 (1959) 6505.
- [36] M. Mégamisi-Bélombé and H. Endres, *Acta Crystallogr., Sect. C*, 39 (1983) 1190.
- [37] M. Mégamisi-Bélombé, P. Singh, D.E. Bolster and W.E. Hatfield, *Inorg. Chem.*, 23 (1984) 2578.
- [38] A. Bencini and D. Gatteschi, *EPR of Exchange Coupled Systems*, Springer, Berlin, 1990.
- [39] W.E. Hatfield, *J. Appl. Phys.*, 52 (1981) 1985, and refs. therein.
- [40] S.S. Eaton, K.M. More, B.M. Sawant and G.R. Eaton, *J. Am. Chem. Soc.*, 105 (1983) 6560.
- [41] G.R. Eaton and S.S. Eaton, *Acc. Chem. Res.*, 21 (1988) 107.
- [42] H. Yokoi and M. Chikira, *J. Am. Chem. Soc.*, 97 (1975) 3975.
- [43] M. Chikira and H. Yokoi, *J. Chem. Soc., Dalton Trans.*, (1977) 2344.
- [44] L.R. Carlin, A. Kopinga, O. Kahn and M. Verdager, *Inorg. Chem.*, 25 (1986) 1786.
- [45] D.K. Towle, S.K. Hoffmann, W.E. Hatfield, P. Singh and P. Chaudhuri, *Inorg. Chem.*, 27 (1988) 394.
- [46] L.N. Kuleshova and P.M. Zorkii, *Acta Crystallogr., Sect. B*, 37 (1981) 1363.
- [47] H. Endres, *Angew. Chem., Int. Ed. Engl.*, 21 (1982) 524.